National Defence
Défense nationale

NEUTRON, ELECTRON AND GAMMA-RAY RADIATION RESPONSES OF A FAST P-I-N PHOTODIODE

by

G.T. Pepper, S.M. Khanna and R.E. Stone

DEFENCE RESEARCH ESTABLISHMENT OTTAWA
REPORT N0. 1237

Canada

November 1994
Ottawa

National Defence Défense nationale

NEUTRON, ELECTRON AND GAMMA-RAY RADIATION RESPONSES OF A FAST P-I-N PHOTODIODE

by

G.T. Pepper, S.M. Khanna and R.E. Stone
Space Systems and Technology Section
Radar and Space Division

DEFENCE RESEARCH ESTABLISHMENT OTTAWA
REPORT N0. 1237

PCN
041LS

November 1994
Ottawa

ABSTRACT

This work is an experimental investigation of radiation-induced changes in the electrical characteristics of the MRD500 P-I-N photodiode, due to various fluences and energies of neutrons, electrons and gamma-rays. Analyses of changes in MRD500 forward bias current-voltage (I-V) characteristics, as a function of fission spectrum neutron fluence (reported as 1 MeV equivalent), indicate that the device can serve as a neutron fluence monitor, useable well beyond the range of the widely-used Harshaw DN-156 P-I-N diode fluence monitors. Furthermore, experimentally-determined changes in MRD500 forward voltage, $\Delta V_F(\phi)$, (at constant I_F and constant temperature) as a function of various energies and fluences of neutrons, electrons and gamma-rays, demonstrate the potential usefulness of the MRD500 as a displacement damage monitor.

In this study, fission neutrons (1 MeV equivalent), 7.5 MeV (average energy) electrons and 1.25 MeV (average energy) gamma-rays are used to investigate the effectiveness of these radiations in producing displacement damage in the MRD500. The device physics responsible for the radiation-induced changes in the electrical characteristics of the diode is also discussed.

RÉSUMÉ

Dans ce travail, nous regardons les changements des caractéristiques électriques des photodiodes P-I-N MRD500 causés par des débits et des énergies différents de neutrons, d' électrons et de rayons gammas. Les analyses des changements des caractéristiques de la polarisation directe courant-voltage (I-V) nous indiquent que les photodiodes MRD500 peuvent servir comme détecteurs de débit des neutrons, et qu'ils sont plus performant que les diodes P-I-N DN-156 de Harshaw. De plus, les variations de la tension directe des diodes MRD500 obtenues en laboratoire, $\Delta V_F(\phi)$, (pour une température et un courant I_F constant), ont démontré que ces diodes ont la capacité d'agir comme détecteurs de défauts de déplacement, pour des débits et des énergies différents de neutrons, d' électrons et de rayons gammas utilisés pour cette expérience.

Dans cette recherche, nous avons utilisés des neutrons (équivalent à 1 MeV), des électrons de 7.5 MeV (moyenne de l'énergie) et des rayons gammas de 1.25 MeV (moyenne de l'énergie) pour étudier (en labratoire) l'efficacité de ces radiations pour produire des défauts de déplacement dans les diodes MRD500. Aussi, nous discutons des attributs physiques des semi-conducteurs (utilisés pour la construction des diodes MRD500) responsables pour les changements des caractéristiques électriques de ces diodes, causés par la radiation.

EXECUTIVE SUMMARY

Radiation damage effects occurring in electronic systems can be accurately characterized only through analyses of the radiation responses of representative "building blocks" of such systems, i.e. P-N and P-I-N junction diodes. Radiation effects in junction diodes can be broadly categorized into two groups, namely ionization (photocurrent) effects and displacement damage effects. In this work, neutron, electron and gamma-ray-induced displacement damage effects in the MRD500 silicon P-I-N photodiode are experimentally investigated. Radiation-induced changes in the measured electrical parameters of the MRD500 are experimentally determined to be related to diode device physics.

Results obtained from analyses of radiation-induced changes in MRD500 diode electrical characteristics indicate that the MRD500 can be used in a variety of applications; as a fission neutron fluence monitor, as a dose rate (photocurrent) calibration device between LINAC electrons and Nd:YAG laser photons, and as a displacement damage monitor for gamma-rays, electrons and fission neutrons, on the range of energies and fluences used in this work.

CONTENTS

LIST OF ILLUSTRATIONS

LIST OF ILLUSTRATIONS (cont'd)

LIST OF TABLES

1.0 INTRODUCTION

Characterization of radiation damage occurring in semiconductor devices and electronic systems is of ongoing interest to researchers in the field of transient radiation effects on electronics (TREE). The P-N junction is one such device that can exhibit permanent deleterious effects due to damage induced by nuclear and space radiation. The P-N junction is one of the simplest (and oldest) active semiconductor devices which finds wide use today in discrete component form, however, the P-N junction also comprises the basic building block for many, more complex semiconductor devices. Devices which inherently rely on P-N junctions for operation are ubiquitous - ranging from bipolar junction transistors (BJTs) to very large scale integrated circuits (VLSICs). Thus, an understanding of how radiation damage affects P-N junctions is a prerequisite to understanding radiation effects in more complex semiconductor devices which utilize P-N junctions. In this work, various radiation-induced changes in the electrical characteristics of the MRD500 P-I-N silicon photodiode are addressed.

In a companion experimental study conducted at DREO[1], several different types of commercially available P-N and P-I-N junction diodes were studied to determine changes in diode electrical characteristics after exposure to fission spectrum neutron fluences ranging from 1E11 to 1E15 neutrons/cm^2 (1 MeV equivalent). In the majority of the devices examined, changes in the post-irradiation electrical characteristics contradicted widely accepted experimental measurements[2-6] of "typical" post-irradiation diode behaviour. An attempt was made to contrast neutron-induced effects with effects produced by "damage-equivalent" fluences of 1.25 MeV (average energy) ^{60}Co gamma-rays (using published damage-equivalence fluence correlations[7,8]), for various P-N junction signal, power, varactor and zener diodes, as well as for P-I-N junction diodes. Again, "atypical" changes in electrical characteristics were evident for many of the examined diodes. Therefore, a specific device that exhibited atypical diode behaviour following irradiation was selected for a series of detailed analyses.

The Motorola MRD500 fast P-I-N photodiode was selected from the group of diodes that exhibited atypical diode behaviour. Changes in the electrical characteristics of MRD500 diodes induced by neutron, electron and gamma-ray irradiation were of interest for a number of reasons. First, since the MRD500 diode was undergoing evaluation[9] at DREO for use as a dose rate (photocurrent) calibration device between 7.5 MeV (average energy) electrons and Nd:YAG laser photons, a complete characterization of the radiation response of the MRD500 would aid in delimiting the useful lifetime of the device, in terms of total dose or fluence of the incident radiation. Second, fast P-I-N junction devices are used in microwave switches or phase-shift arrays[4,10]. Since switching times of such devices are known to change following irradiation, and since the MRD500 is technologically representative of these devices, then an examination of the radiation induced electrical changes the in MRD500 (under both DC and AC conditions) was deemed important. Third, cursory examination of MRD500 response to neutrons (1 MeV equivalent) suggested that this device could prove useful as a neutron fluence monitor, extending the fluence measurement range of the widely-used Harshaw DN-156 P-I-N diodes. As the MRD500 is currently a small fraction of the cost of the Harshaw product, then the importance of this potential application could not be left unaddressed. Finally, examination of the radiation response of the MRD500 diode provided an opportunity to investigate the equivalence of neutron, electron and gamma-ray-induced displacement damage effects on several of the important electrical characteristics of the device.

2.0 DESCRIPTION OF P-I-N JUNCTIONS

2.1 P-I-N JUNCTION OPERATION

A silicon P-I-N junction can be described as a P-N junction[2-5] with a layer of intrinsic silicon positioned between P- and N-type extrinsic layers, as shown in figure 1. Under either DC bias conditions or low frequency AC bias conditions, P-I-N junctions exhibit I-V characteristics approaching that of ideal P-N junctions; negligible resistance when forward biased and very high resistance when reverse biased. For the P-I-N junction, however, not only does the high resistance intrinsic layer (base region) enable the junction to withstand higher levels of reverse bias than can similarly constructed and biased P-N junctions, but the increased width of this region results in a higher junction breakdown voltage. Since the base region acts like a variable length resistor, the P-I-N junction can be described as a P-I junction in series with a resistor and an I-N junction. The P-I junction behaves exactly like a P^+N junction in which the N-type silicon is very lightly doped, while the I-N junction behaves exactly like a N^+P junction in which the P-type silicon is very lightly doped.

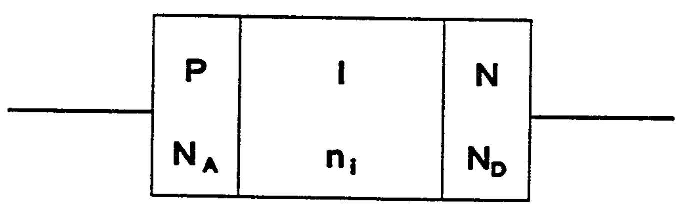

Figure 1 : **Typical P-I-N junction diode structure.**

The P-I-N junction is formed when majority carriers (holes) in the P-type silicon near the P-I junction diffuse into the base region, while majority carriers (electrons) in the N-type silicon near the I-N junction diffuse into the base region. This diffusion forms two regions of ionized acceptor atoms (N_A) and ionized donor atoms (N_D), or two "space charge" regions; an ionized acceptor/donor region at the P-I interface and an ionized acceptor/donor region at the I-N interface, respectively. The electric fields associated with these space charge regions give rise to potential differences across the P-I and I-N junctions. Current flow under reverse and/or forward bias at the former is due mainly to holes, while at the latter it is due mainly to electrons.

Characteristic current-voltage (I-V) equations for unirradiated P-I-N junction diodes operating under low-level injection are well known and appear in Appendix A. The radiation responses of P-I-N junction diodes are introduced in section 2.2.

2.2 P-I-N JUNCTION RADIATION RESPONSE

Radiation effects produced in P-N and P-I-N junction diodes are of two types; photocurrent (ionization) effects and displacement damage effects[11]. Total dose effects (excluding displacement damage) are not applicable due to the structure and physics of operation of the devices. The absence of an insulating oxide layer precludes the possibility of charge trapping occurring within P-N and P-I-N junction devices.

In the absence of catastrophic device damage (e.g. device burn-out) due to excessive current flow through the P-N junction, photocurrent effects are non-permanent. Given appropriate electrical conditions, electron-hole pairs (ehp's) created through ionization in the vicinity of the P-N junction region can give rise to a photocurrent. The radiation-induced photocurrent decays very rapidly to zero once the incident ionizing radiation has ceased.

Displacement damage effects are changes in device electrical characteristics that occur when semiconductor atoms are displaced from their equilibrium lattice positions by energetic radiation. The magnitude of these effects depends upon such factors as the type, energy and fluence of the incident radiation, and the type of semiconductor material in the active region of the device undergoing irradiation (e.g. Si, GaAs, etc.). Displacement damage effects can be both temporary (i.e. via annealing of defects) and permanent.

Gamma-rays directly produce only ionization effects in semiconductor materials and can create displacement damage only via indirect means. Gamma-rays interacting with the atoms in the semiconductor lattice can liberate energetic free electrons (via Compton scattering and pair production) which may possess sufficient kinetic energy to subsequently cause displacement damage via electron/nucleus collisions. Device irradiation with electrons directly produces both ionization effects and displacement damage effects. Irradiation with neutrons primarily produces displacement damage in junction devices. [Note, however, that energetic recoil nuclei and charged particles created via (n,x) reactions can produce significant ionization along their tracks before coming to rest.]

For silicon at room temperature, the majority of displacement "defects" (i.e. interstitial atoms and lattice vacancies, somewhat analogous to electrons and holes, respectively) are relatively mobile and either recombine directly, or with impurities resident in the semiconductor material lattice prior to irradiation[11]. A considerable fraction of the total number of defects produced recombine at room temperature, within milliseconds of formation. This initial recombination of defects is known as the (room-temperature) "short-term annealing" behaviour of the device under analysis. Prolonged annealing at room temperature on the order of days, or "long-term annealing", can reduce defect concentrations to a small fraction of the number remaining after the completion of short-term annealing[11]. Annealing effects in MRD500 diodes are discussed in section 3.2.

Extensive experimental work on displacement-induced changes in the electrical characteristics of "typical" or "wide-base" P-I-N junction diodes can be found in the literature[6,12-14]. Generally, these devices exhibit pre- and post-irradiation characteristics illustrated in figure 2. Displacement defects produced during irradiation act either as recombination centres or as generation centres (under forward or reverse bias, respectively) for excess carriers, thereby reducing effective carrier lifetimes in the diode. In response, as fluence increases, diode forward bias voltage increases for constant forward current, diode reverse current increases in magnitude for constant reverse bias voltage, and diode breakdown voltage increases in magnitude. Diode capacitance decreases[12,15-17] as both reverse bias voltage and frequency increase, provided that the voltage remains below the voltage required to fully deplete the space charge region of the diode[13,14]. Device switching times generally decrease, in response to decreased junction capacitance of the device.

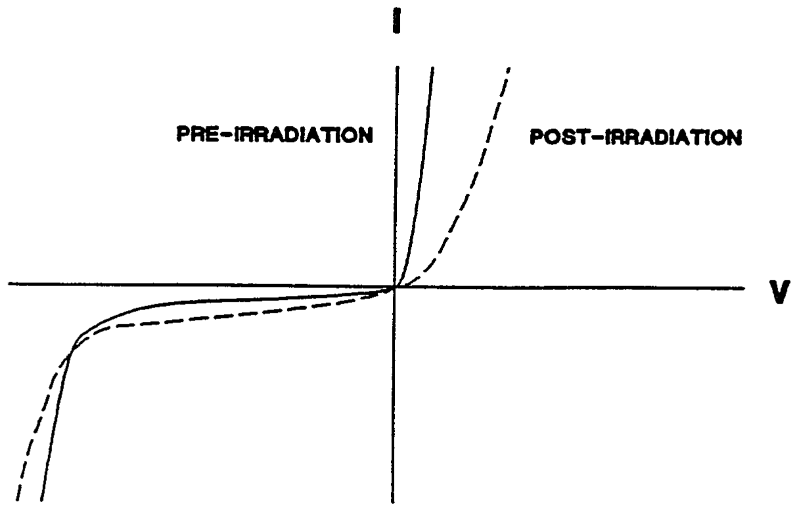

Figure 2 : **Pre- and post-irradiation I-V characteristics of typical P-I-N junction diodes.**

Limited information is available in the literature[4,10], however, regarding changes in the I-V characteristics of forward and reverse biased, abrupt junction, narrow-base, fast P-I-N diodes (i.e. MRD500 diodes) resulting from displacement damage induced by exposure of diodes to energetic neutrons, electrons and gamma-rays. Generally though, in such a device, for $N_D > N_A$ and $V_F > 8kT/q$, the diode forward current, I_F , is

$$I_F = \frac{qAn_i^2\sqrt{D_e}}{N_A\sqrt{\tau_e}}\exp\left(\frac{qV_J}{kT}\right) \tag{2.1}$$

with terms defined as per Appendix A, and with

D_e , τ_e = diffusion coefficient and carrier lifetime, respectively, for electrons.

Equation (2.1) can be rearranged to show

$$V_J = \frac{kT}{q} \ln\left[\frac{I_F N_A \sqrt{\tau_e}}{qAn_i^2\sqrt{D_e}}\right] \tag{2.2}$$

Displacement defects created during irradiation of the diode act as recombination centres and cause τ_e to decrease in the diode[4-6,10]. As a result, the voltage drop across the junction, V_J, must decrease relative to the pre-irradiated value, for constant I_F and ambient temperature. The total forward voltage drop across the diode, V_F, is described by

$$V_F = V_J + V_B \tag{2.3}$$

For a very narrow base region, the resistive component, V_B, of V_F is relatively low, since the resistance of the base region of the diode is proportional to the width of the base. Hence, inspection of equation (2.3) shows that V_J necessarily dominates V_F. As radiation fluence increases, however, a fluence/damage level is reached at which even a narrow-base diode sustains enough material damage to noticeably increase the resistance of the base region (and therefore, V_B), through production of very high concentrations of displacement induced defects in the semiconductor lattice and the resultant decrease in carrier mobility. At this juncture, V_B exceeds V_J and therefore, begins to dominate V_F. This behaviour can be observed in figure 3.

For an unirradiated, reverse biased, abrupt junction, narrow-base P-I-N diode, with $N_D > N_A$, and where $V_R \leq -4kT/q$ ($\approx$ −100 mV at room temperature), the diode current is described by

$$I_R = qAn_i^2\left(\frac{\sqrt{D_e}}{N_A\sqrt{\tau_e}}\right) \tag{2.4}$$

As the voltage dependence of I_R has been removed, I_R has "saturated" at I_S and will remain relatively constant until V_R approaches the breakdown voltage for the device[2,3]. Also, since an increase in radiation fluence delivered to the diode causes a commensurate decrease in carrier lifetime, close inspection of equation (2.4) reveals that as fluence increases, one can expect to observe a net monotonic increase in the magnitude of I_R (at constant V_R). This behaviour can also be observed in figure 3.

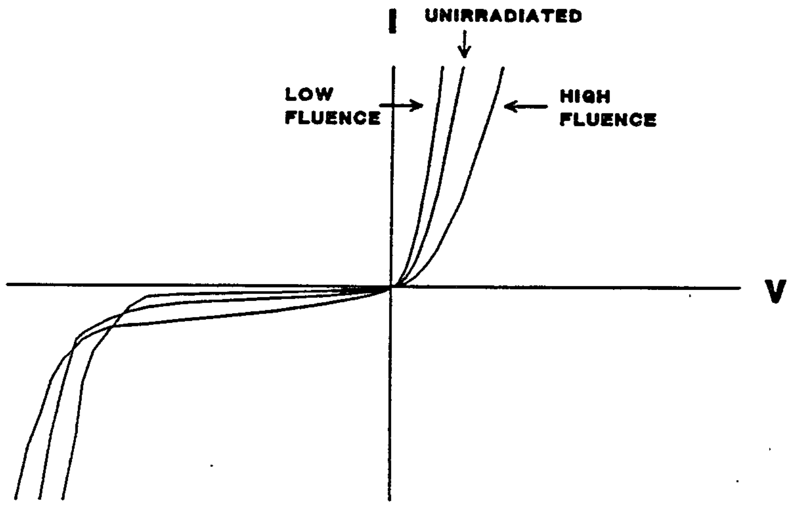

Figure 3 : **Pre- and post-irradiation I-V characteristics of abrupt junction, narrow-base P-I-N diodes.**

Changes in V_{BR} , C-V, and C-f characteristics of MRD500 diodes are addressed in sections 4.3 through 4.5.

3.0 EXPERIMENTAL

3.1 DESCRIPTION OF THE MRD500 P-I-N JUNCTION DIODE

The Motorola MRD500 is a fast P-I-N photodiode[18] with a sub-nanosecond rise time, shown schematically in figure 4. The small junction area of the device is indicative that the MRD500 has a relatively low junction capacitance (typically ≤ 5 to 10 picofarads) and a correspondingly fast rise time. The figure also defines that $N_D > N_A$ (electron-type conduction) for the device, and describes the relatively narrow base region width (25 μm) of the junction of the MRD500[19]. While base widths of wide-base P-I-N junction devices are on the order of hundreds of micrometers (μm)[2,3,12-14], however, the base width of the MRD500 junction is markedly less. Therefore, the resultant high carrier concentration gradient developed across the narrow junction region infers that the MRD500 is an abrupt junction, narrow-base P-I-N diode.

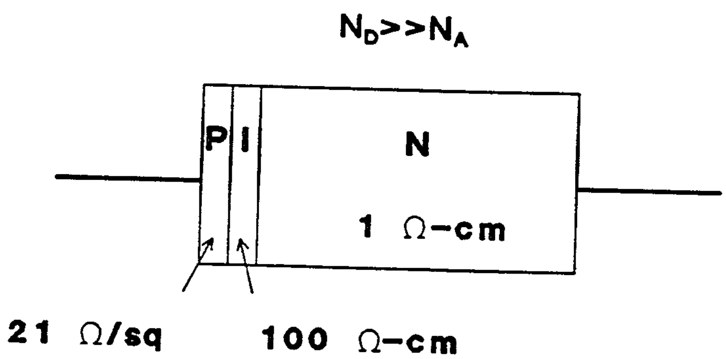

Figure 4 : **Junction schematic of MRD500 P-I-N diode.**

3.2 GENERAL MEASUREMENT TECHNIQUES

MRD500 diodes used in this work were procured from the same production lot, in an attempt to minimize device-to-device variations in electrical characteristics. All devices were irradiated with the junctions short-circuited, to obviate photocurrent and static-discharge damage. The lenses of all devices were rendered opaque prior to acquisition of electrical measurements.

Each reported datum represents the average value of measurements made for four separate devices. In an attempt to minimize any variation in thermal annealing effects, devices were measured both pre- and post-irradiation at approximately 25°C, and were maintained as close as possible to this temperature during the irradiations. Device I-V data were acquired with an IBM PC/AT linked via an HPIB interface to a Hewlett-Packard HP4145B semiconductor parameter analyzer. Importantly, forward bias voltage ranges were selected to ensure that $V_F > 8kT/q$, but to simultaneously limit I_F to 2.0 mA maximum, an empirically-determined maximum value for I_F below which current-induced annealing effects in MRD500 diodes were observed to be insignificant.

Device V_{BR} measurements were performed, using an Ortec 456 high voltage power supply to bias the devices, a Keithley 619 electrometer/multimeter to monitor device reverse current and a Fluke 87 multimeter to monitor device V_{BR}. Capacitance versus frequency and C-V data were obtained with a Hewlett-Packard HP4192A low frequency impedance analyzer.

Electrical measurements on electron and gamma-ray irradiated devices were conducted one hour following irradiation. Neutron irradiated devices were measured approximately one month following removal from the source (refer to section 3.3). The measurement delay period was required for neutron activation products to decay sufficiently to permit safe handling. While electron and gamma-ray irradiated samples showed evidence of short-term annealing, minimal long-term annealing was observed for neutron, electron and gamma-ray irradiated devices.

3.3 NEUTRON MEASUREMENTS

Neutron irradiation of MRD500 diodes was performed at the Army Pulse Radiation Facility (APRF), U.S. Army Combat Systems Test Activity (USACSTA), Aberdeen Proving Ground, Maryland. Five separate packages containing four MRD500 diodes each were assembled, with the diodes mounted on electrically-conductive (e.g. antistatic) foam bases. The packages were placed successively at the bottom of the 1.5 inch "glory hole" of the APRF core, for durations appropriate to deliver fission neutron fluences (1 MeV equivalent) ranging from 1E11 to 1E15 n/cm^2, in order-of-magnitude fluence increments. Gamma-ray dosimetry was performed by mounting both CaF_2:Mn thermoluminescent detectors (TLDs) on either side of the midline of the samples, at the bottom of the glory hole. Neutron dosimetry was performed using sulphur activation detectors. Forced-air cooling of the glory hole was performed to maintain sample temperatures at approximately 25°C. The overall uncertainty in reported neutron fluences[20] is estimated to be ± 10%.

3.4 ELECTRON MEASUREMENTS

Irradiation of MRD500 diodes was performed using the MEVEX electron linear accelerator (LINAC), in Stittsville, Ontario, with various fluences of 7.5 MeV (average energy) electrons. Estimates of the fluence of 7.5 MeV electrons required to produce displacement damage in Si equivalent to that created by a given fluence of fission neutrons were obtained from published displacement damage correlations[7]. This step was used only to reduce the total number of device irradiations performed, and was not a prerequisite for any of the results presented in this work.

Groups of four diodes were mounted in a water-cooled test jig and were subsequently irradiated for durations appropriate to deliver electron fluences ranging from 4E12 to 4E16 e/cm^2, in order-of-magnitude fluence increments. Devices were irradiated with the surface of the semiconductor die oriented perpendicular to the electron beam. To ensure that a constant electron fluence was received by all diodes used in each separate irradiation, MRD500 diode irradiations were performed only following determination of the central axis of the electron beam and optimal placement of the diode test jig.

A Faraday cup was used to integrate the electron fluence directly behind the target on the central axis of the electron beam. Far West Technologies FWT 60-00 radiachromic nylon films were used to verify the spatial uniformity of the beam in the irradiation plane containing the devices under test (DUT). The uncertainty in the reported electron fluence values is estimated to be ±15%, containing error contributions from (a) the value of the integrated charge obtained with the Faraday cup, (b) the small spatial variation of the electron fluence delivered to the DUT, and (c) the unavoidable modification of the detected fluence introduced by insertion of the DUT in front of the Faraday cup.

3.5 GAMMA-RAY MEASUREMENTS

Gamma-ray irradiation of MRD500 diodes was performed at DREO, using the 6,510 Ci AECL GB-150C ^{60}Co source. The source facility is well characterized in terms of exposure rate (in air) versus distance, and this data was used to calculate the fluences of 1.25 MeV (average energy) gamma-rays incident on DUT. Estimates of gamma-ray fluences required to produce varying levels of displacement damage in Si were obtained from published displacement damage correlations[7]. Similar to the electron irradiations of section 3.4, this step was used only to reduce the total number of device irradiations performed, and was not a prerequisite for any of the results presented in this work.

Separate groups of four diodes were mounted on electrically-conductive foam pads and placed in a test jig, with the devices oriented such that the incident gamma-ray flux was perpendicular to the surface of the semiconductor die. Devices were then irradiated at a source-DUT distance of 10.0 ± 0.1 cm (an exposure rate ≈ 5,300 R/hr), for durations appropriate to supply 1.25 MeV gamma-ray fluences ranging from 3E11 to 3E15 γ/cm^2, in order-of-magnitude fluence increments. Far West Technologies FWT 60-00 radiachromic nylon films were used to verify the spatial uniformity of the beam in the irradiation plane containing the DUT.

The overall uncertainty in reported values of gamma-ray fluences delivered to MRD500 diodes is estimated to be ± 5%, attributable mainly to test jig positioning errors. The relatively small source-DUT distance was required to ensure that desired gamma-ray fluences were acquired with reasonable exposures, i.e. within several days.

To obtain the fluence estimates discussed above, and to ensure that the experimental measurements of the damage equivalence of various types and energies of radiation could be compared with published data[7], the gamma-ray energy deposited as a function of depth in the MRD500 diodes was required. [Charged particle equilibrium doesn't exist due to the thickness of the device.] The ITS (Integrated Tiger Series) photon/electron Monte Carlo radiation transport code was used to produce the required depth-energy deposition profile data. For the ITS simulation, 1.25 MeV photons were made normally incident upon an infinite surface area, 250 μm-thick slab of Si (equal to the thickness of the die of the MRD500 diode[19]). The semiconductor slab was subdivided into 10 layers, each 25 μm thick, so that the absorbed dose in the first two layers (corresponding to the junction region of the MRD500) could be explicitly determined. The results of this simulation (for 2E7 photon histories) appear in figure 5. Note that the depth-dose profile has been normalized to one incident particle (i.e. MeV cm^2/g per source particle), therefore, conversion from fluence to energy deposition is straightforward. The energy deposited per photon in the entire thickness of the device (2.85E-3 MeV) corresponds to 0.23% of the incident photon maximum energy (1.25 MeV).

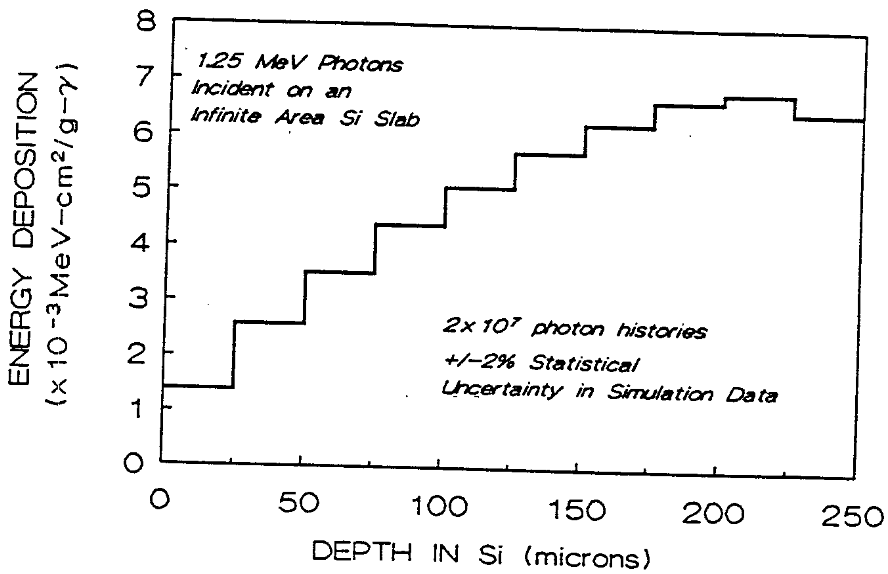

Figure 5 : **Depth-dose profile for 1.25 MeV gamma-rays normally incident upon an infinite-area, 250 μm-thick Si slab.**

3.6 CARRIER LIFETIME MEASUREMENTS

Measurements of pre- and post-irradiation carrier lifetimes in junction diodes can be used to quantify radiation-induced displacement damage in semiconductor devices[4-6,10]. Therefore, MRD500 diode pre- and post-irradiation carrier lifetime measurements were made to provide support for experimental damage correlations developed from MRD500 I-V measurements.

Lifetime ("τ") measurements were performed for pre-irradiated diodes, as well as for diodes irradiated at various neutron, electron and gamma-ray fluences using the refined step-recovery technique of Dean et al[21]. The technique involves measuring the transient response of an initially forward biassed junction to a sudden reversing step potential. The technique is applicable to P-N junctions with nearly arbitrary impurity distributions and can achieve a temporal resolution of better than 1 nanosecond. Measurements were obtained using a Tektronix 7912HB programmable digitizer, a Hewlett-Packard HP8008A pulse generator, several Hewlett-Packard signal attenuators, and a Philips PM3267 fast oscilloscope. Diodes used in the lifetime measurements were taken from a common production lot. Results of the carrier lifetime measurements are discussed in section 4.6.

4.0 RESULTS AND ANALYSES

4.1 FORWARD CURRENT VS. VOLTAGE

4.1.1 **Changes in Forward Voltage:** Figure 6 shows measured pre- and post-irradiation forward bias I-V characteristics observed for neutron irradiated MRD500 diodes. The uncertainty in all the reported I-V data is estimated to be less than ± 5%. Results obtained for gamma-ray irradiated and electron irradiated diodes exhibit similar trends but are not shown, due to the volume of data.

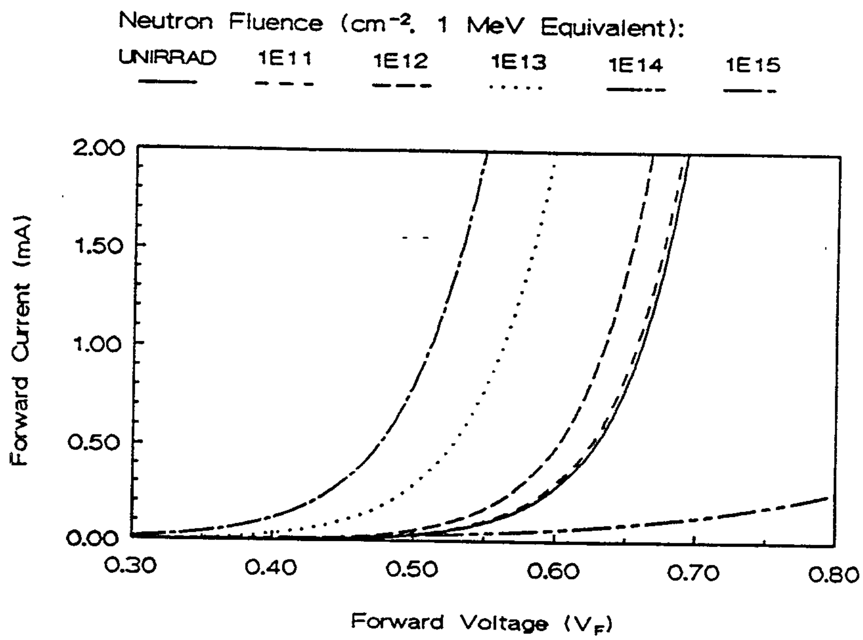

Figure 6 : **Forward I-V characteristics of MRD500 diodes before and after irradiation with cited fluences of (1 MeV equivalent) fission neutrons.**

Trends observed in the I-V behaviour of neutron, electron and gamma-ray irradiated diodes shown in figure 6 can be compared by selecting a common I_F and observing fluence-induced changes in diode V_F characteristics at this current. A more direct interpretation of the forward bias I-V behaviour of MRD500 diodes can be obtained from figure 7. This figure indicates that with I_F = 0.4 mA, for example, for neutron, electron and gamma-ray irradiated diodes, V_F values decrease linearly and monotonically from unirradiated diode values at low fluence levels, but then begin to increase monotonically once a particular fluence level is exceeded, surpassing eventually even the unirradiated diode V_F values. In this work, the fluence at which V_F attains a minimum value is referred to as the "reversal" fluence for the MRD500, for a specific type and energy of irradiating particle.

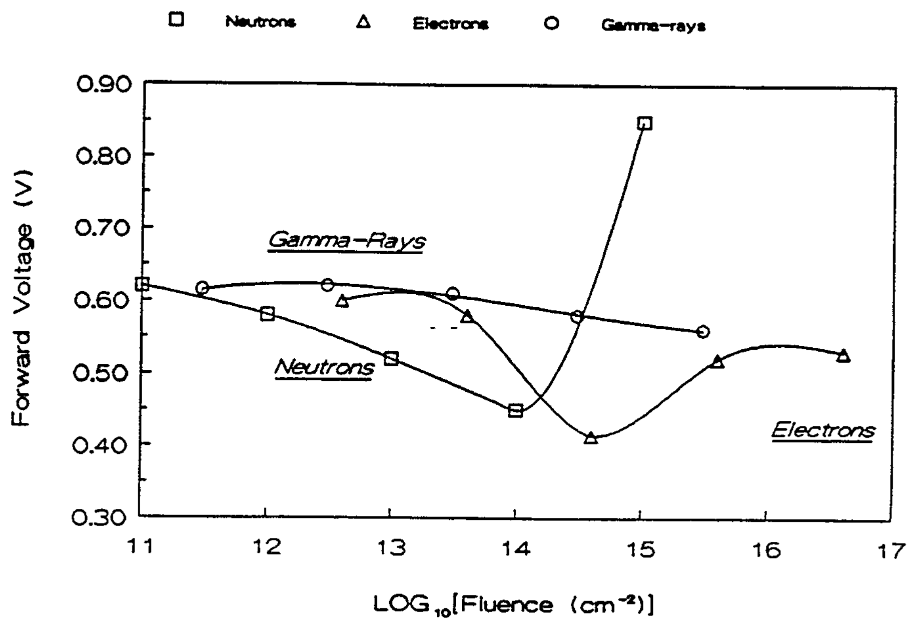

Figure 7 : **MRD500 forward voltage as a function of particle fluence, for diodes irradiated with neutrons, electrons and gamma-rays; I_F = 0.40 mA.**

Figure 7 indicates a reversal electron fluence of slightly greater than 4E14 e/cm^2 and a reversal neutron fluence located between 1E14 and 1E15 n/cm^2. This general behaviour is explained in section 2.2. Essentially, since carrier lifetime decreases[4-6,10] as radiation fluence increases, equation (2.2) shows that V_J decreases as fluence increases, up to the reversal fluence. Since radiation-induced increases in the resistance of the base material of the diode are minimal for low fluences, then equation (2.3) indicates that V_J dominates V_F and hence, V_F decreases linearly and monotonically as fluence increases monotonically, up to the reversal fluence (at a constant I_F and temperature). At the reversal fluence, however, V_F decreases to a minimum value and then begins to increase monotonically, since radiation-induced increases in R_B become significant and therefore, V_B begins to dominate V_F.

Specifically, figure 6 indicates that diode base resistance ($R_B \approx$ inverse slope of the I-V curve) changes very little with fluence (at constant I_F), up to the reversal fluence. Below the reversal fluence, the relatively low value observed for R_B suggests that radiation-induced displacement damage in the base of the diode remains low and constant. However, R_B is observed to increase rapidly and monotonically with fluence once the reversal fluence is surpassed, due to increased concentrations of radiation-induced displacement defects in the bases of the diodes. Therefore, beyond the reversal fluence, radiation-induced changes in V_F are dominated by associated changes in V_B. Importantly, the pre-reversal fluence invariance of R_B points to the linear nature of $\Delta V_F(\phi)$, for $\phi < \phi_{REVERSAL}$.

Figure 7 shows that gamma-ray fluences used to irradiate the MRD500 diodes were less than that required to reach the reversal fluence. Also, the figure shows data for 3E11 and 3E12 γ/cm^2 irradiations that contradict trends observed for results observed at other gamma-ray fluence levels. Although both of these exceptions in the data remain unexplained, gamma-ray fluences delivered to the diodes were based upon predictions[7,8] generated from analyses of neutron and proton displacement damage-induced changes in the gain (h_{fe}) of a bipolar transistor, rather than ΔV_F for a P-I-N diode. Hence, direct application of the h_{fe}-based damage correlations to predict neutron and electron equivalent fluences in MRD500 P-I-N photodiodes may not describe completely the effects of gamma-rays in these devices.

4.1.2 **Displacement Damage Correlations:** Silicon displacement damage factor ratios (K/K_n; where K is a composite displacement damage factor for the type and energy of radiation of interest, and K_n is that K for neutrons) extracted from the literature[7] have been used to obtain estimates of the equivalence of production of displacement damage in silicon, for neutrons, electrons and gamma-rays. Electron and gamma-ray fluences used in the experiments were selected to produce the same degree of displacement damage as given fluences of neutrons (1 MeV equivalent). Changes in V_F (at constant I_F and temperature) for a variety of diodes have been shown to be proportional to displacement damage produced by incident particle fluences[6,23], therefore, the results obtained from an experimental analysis of different types and energies of radiation required to produce the same ΔV_F can be used to generate experimental displacement damage correlations for MRD500 diodes. Note that damage factor ratio (K/K_n) data[7], presented elsewhere, was obtained by measurement of changes in h_{fe} of a silicon bipolar transistor following device irradiation with a wide range of fluences and energies for fission neutrons, electrons, and protons.

Figure 8 illustrates the proportionality between device damage and the change in forward voltage, ΔV_F, where ΔV_F (mV) is plotted against irradiating particle fluence (cm^{-2}) for particle fluences below the reversal fluence. From the experimental results, the ratio of fluences of 7.5 MeV electrons to fission neutrons (1 MeV equivalent) required to produce a −40 mV shift in V_F (for I_F = 0.4 mA) is approximately 26:1. Therefore, since damage is proportional to the measured shift in V_F, neutrons (1 MeV equivalent) are approximately 26 times more effective than 7.5 MeV electrons, per unit fluence, in producing displacement damage in MRD500 diodes. For comparison, published experimental data[7] indicates that fission neutrons (1 MeV equivalent) are approximately 20 times more effective than 7.5 MeV electrons (per unit fluence) in producing displacement damage in silicon, in excellent agreement with the experimental results of figure 8.

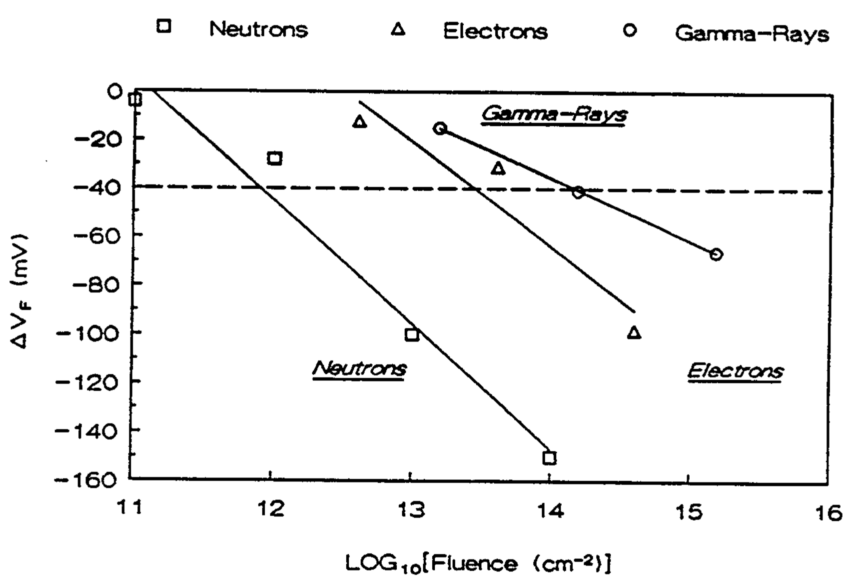

Figure 8 : **Change in V_F with particle fluence, for MRD500 diodes irradiated with neutrons, electrons and gamma-rays; I_F = 0.40 mA.**

Figure 8 also shows that the observed ratio of fluences of 1.25 MeV gamma-rays to 1 MeV equivalent fission neutrons required to produce a -40 mV shift in V_F (for I_F = 0.4 mA) is approximately 140:1, while published experimental data[7,8] indicate that 1 MeV equivalent fission neutrons are approximately 100 times more "effective" than 1.25 MeV gamma-rays (per unit fluence) in producing displacement damage in silicon. Again, reference data are in good agreement with the experimental results of figure 8. Results for I_F = 0.8 mA through 2.0 mA were compiled and exhibit similar trends.

Importantly, figures 6, 7 and 8 show that MRD500 diodes display relatively high, linear $\Delta V_F(\phi)$ sensitivity, up to and including neutron-equivalent fluences of 1E14 cm^2, well beyond the useable fluence measurement range of the Harshaw damage monitor P-I-N diodes.

4.2 REVERSE CURRENT VS. VOLTAGE

Figure 9 shows the pre- and post-irradiation reverse bias raw I-V characteristics measured for neutron irradiated MRD500 diodes used in the experiments. Results obtained for gamma-ray irradiated and electron irradiated diodes exhibit similar trends but are not shown, due to the volume of data. Trends observed in the I-V curves for neutron, electron and gamma-ray irradiated diodes can be compared by selecting a common V_R and observing changes in diode characteristics at this voltage. For example, figure 9 shows that for V_R = -20.0 V, the magnitude of I_R increases monotonically but non-linearly for all neutron fluences delivered to the diodes. Also, the figure shows that values obtained for I_R (at constant V_R and temperature) span approximately six orders of magnitude. This behaviour is explained in detail in section 2.2. Similar trends have been reported and discussed elsewhere in the literature[4-6,10-12,17].

Since radiation-induced displacement damage is proportional to the change in reverse current (at constant V_R), a plot of ΔI_R versus particle fluence, ϕ , will yield a damage correlation for neutrons, electrons and gamma-rays. However, correlation results are shown only for MRD500 forward characteristics, for two reasons. First, figure 9 indicates that for the range of types and energies of fluences used in the experiments, ΔV_F is linear with the associated change in fluence, $\Delta\phi$, while ΔI_R is not. Second, the precision associated with acquisition of millivolt changes in V_F is much higher than the precision associated with acquisition of picoampere changes in I_R , especially when picoampere ΔI_R values span approximately seven orders of magnitude.

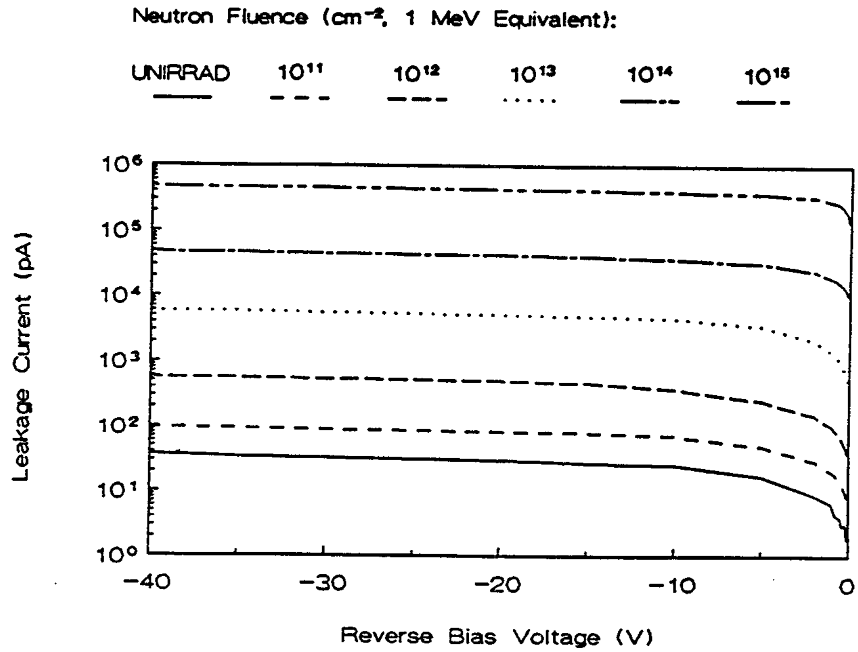

Figure 9 : **Reverse I-V characteristics of MRD500 diodes before and after irradiation with fission neutrons (1 MeV equivalent).**

4.3 REVERSE BREAKDOWN VOLTAGE

Breakdown-region pre- and post-irradiation I_R versus V_R characteristics of neutron irradiated MRD500 diodes are shown in figure 10. To reduce the possibility of damaging devices through the application of high V_R prior to irradiation, V_{BR} results shown are for unirradiated diodes and represent average measurements made for four diodes taken from the same production lot as all the irradiated diodes. The variation in averaged V_{BR} values for unirradiated diodes was typically ± 7% from the mean value. The uncertainty in all measured values is estimated to be ± 5%.

Explicitly, it can be seen that the magnitude of V_{BR} increases monotonically with neutron fluence, changing approximately 40 volts for an associated fluence increase from 1E11 to 1E15 n/cm^2. Results for gamma-ray irradiated and electron irradiated MRD500 diodes exhibit similar trends but are not shown, due to the volume of data. Pre- and post-irradiation V_{BR} characteristics shown in figure 10 are explained in the literature[2-4].

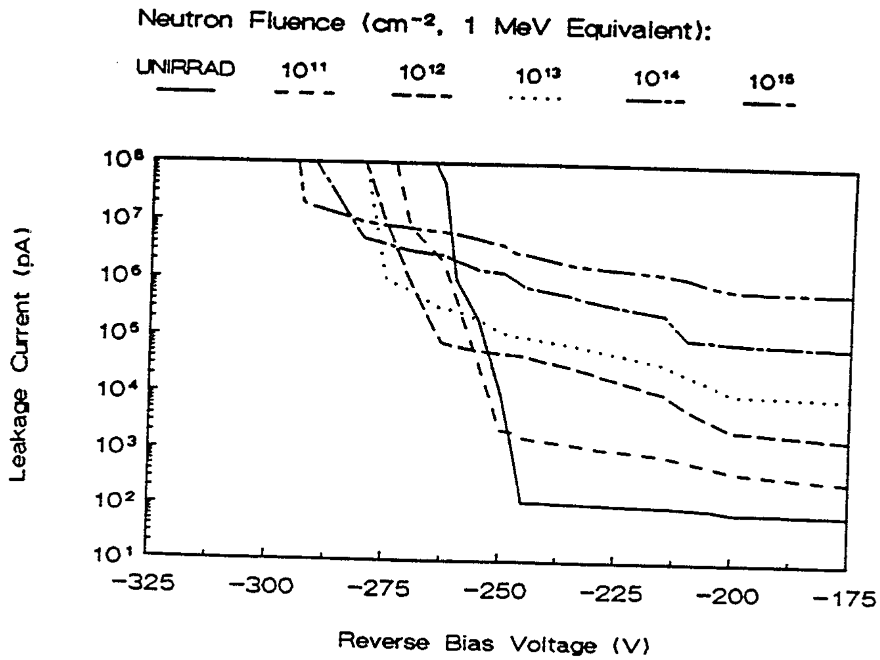

Figure 10 : **Reverse breakdown voltage for MRD500 diodes before and after neutron irradiation.**

Explanation of the V_{BR} behaviour of the MRD500 diode is based upon the fact that the MRD500 is an abrupt junction, narrow-base P-I-N diode, with $N_D > N_A$. Therefore,

$$V_{BR} = \frac{\epsilon_S E_{CRIT}^2}{2qN_D} \tag{4.1}$$

where

ϵ_S = dielectric constant of the semiconductor material in the device

E_{CRIT} = the depletion region electric field required to produce avalanche breakdown in the device.

Changes in post-irradiation V_{BR} characteristics of the MRD500 depend upon the existing donor impurity level in the semiconductor, N_D , and the magnitude of the critical electric field, E_{CRIT} , for the device[6]. Radiation-induced production of ehp's causes effectively a monotonic "reduction" in post-irradiation values of N_D (due to recombination), with increasing fluence. Hence, the breakdown voltage of the device increases monotonically with fluence. Generally speaking, however, V_{BR} values found for P-I-N diodes are also highly dependent upon the width of the high resistivity base region (relative to the N- and P-type regions) of the devices. Wide-base P-I-N diodes are able to withstand very high reverse bias voltages (typically on the order of 1 kV) before E_{CRIT} becomes high enough to initiate avalanche breakdown. Abrupt junction, narrow-base diodes such as the MRD500 can withstand relatively low (typically on the order of 100 to 400 V) reverse bias voltages before V_{BR} is reached.

4.4 CAPACITANCE VS. VOLTAGE

Typical high-frequency (1 MHz) pre- and post-irradiation C-V characteristics of gamma-ray irradiated MRD500 diodes appear in figure 11. Results shown in the figure as unirradiated values represent an average of four diodes taken from the same production lot as the irradiated diodes. The variation in averaged C-V measurements performed on unirradiated diodes was typically ± 5% from the average. The uncertainty in C-V data measured for irradiated diodes is estimated to be ± 10%.

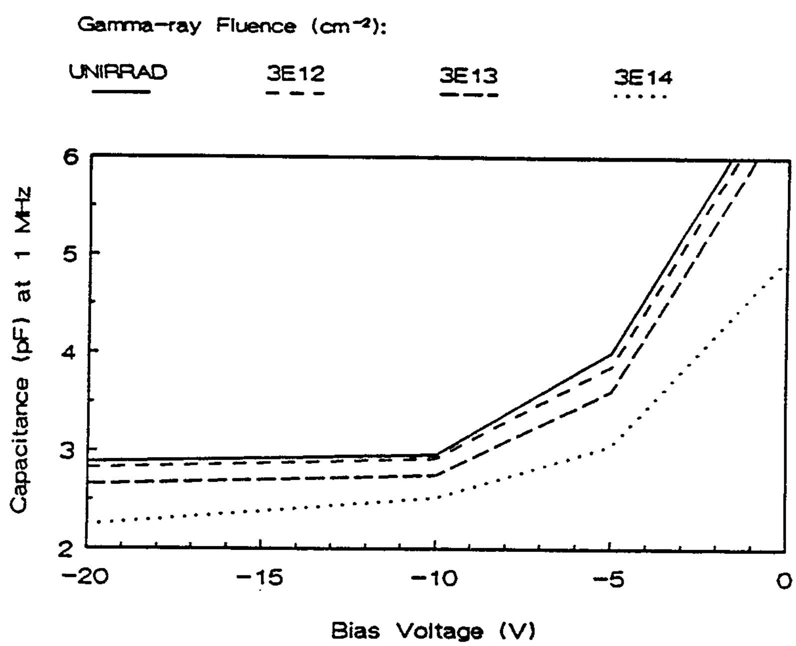

Figure 11 : **Capacitance-voltage characteristics of MRD500 diodes at 1 MHz, before and after gamma-ray irradiation.**

Figure 11 shows that for a given gamma-ray fluence, and with $V_R \leq -10$ V, MRD500 diode capacitance remains relatively constant as V_R increases. For $V_R \geq -10$ V, the figure indicates that at constant fluence, capacitance varies roughly as V^{-2}. For low fluences, MRD500 post-irradiation C-V characteristics remain relatively unchanged from pre-irradiation characteristics. Conversely, the figure indicates that at high fluence levels ($\phi \geq$ 3E14 γ/cm^2), with $V_R \leq -10$ V (approximately), diode capacitance apparently saturates, changing slowly as V_R increases. Results for electron and gamma-ray irradiated diodes exhibit similar trends.

Experimental data presented in figure 11 are consistent with results reported previously in the literature[10,12,15,16]. Space charge layers formed at both the P^+N and N^+P junctions of the MRD500 diode contain relatively few free carriers, therefore, they behave like insulators of dielectric constant ϵ_S, approximately equal to that of the base region of the device[2,3]. Introduction of relatively high impurity concentrations into the P-type and N-type regions of the diode (with respect to the base region), cause the conducting P-type and N-type sections of the reverse biased device to behave like the plates of a parallel-plate capacitor. Thus, the space charge layers and the base region behave like a capacitor of plate area A_J, dielectric thickness W, and dielectric constant ϵ_S. The resultant junction capacitance is

$$C_J = \frac{\epsilon_S A_J}{W} \qquad (4.2)$$

provided that V_R is large enough to fully deplete the base region of free carriers. Under these circumstances, the P-I-N diode behaves like a voltage-independent, fixed-capacitance, parallel-plate capacitor. This behaviour is observed in figure 11, for $V_R \leq -10$ V.

When V_R is not large enough to fully deplete the base region, the dielectric thickness changes with applied voltage and the junction capacitance becomes[2,3]

$$C_J = \sqrt{\frac{q\epsilon_S (N_D - N_A)}{2\,(V_R + V_{BI})}} \qquad (4.3)$$

where

V_{BI} = "built-in" voltage of the P-I-N junction.

Equation (4.3) indicates that the pre-irradiation reverse bias capacitance of an undepleted typical P-I-N junction device exhibits a $V_R^{-0.5}$ dependence (for $V_{BR} > V_{BI}$), thereby supporting experimental results obtained from figure 11, when $V_R \geq -10$ V. Since the capacitance of unirradiated MRD500 diodes is observed to be independent of voltage for $V_R \leq -10$ V, then MRD500 diode depletion voltage, $V_{DEPL} \approx -10$ V.

The post-irradiation reverse bias capacitance of a typical P-I-N junction diode depends upon reverse bias voltage strength and frequency, and the magnitude of the incident radiation fluence (for a given type and energy of radiation). At relatively low fluences, little damage is created within the device and post-irradiation C-V characteristics remain relatively unchanged from pre-irradiation characteristics[10,16]. However, at constant frequency and for moderate fluence levels (up to 3E14 γ/cm^2 in low resistance substrates), creation of defects near the periphery of the "dielectric region" of the "junction capacitor" causes moderate lengthening of the dielectric region[12]. Subsequently, C_J decreases as ϕ increases. For high fluence levels, dielectric region lengthening and large increases in $(N_D - N_A)$ effectively saturate C_J, removing the voltage dependence of C_J. Figure 11 shows the effective saturation of C_J, for $V_R \leq -8$ V and with ϕ = 3E14 γ/cm^2.

4.5 CAPACITANCE VS. FREQUENCY

Pre-and post-irradiation C-f characteristics of the MRD500 diode (measured at several reverse bias voltages) appear in table 1, as well as in figures 12 and 13. Tabulated pre-irradiation C-f characteristics measured for gamma-ray irradiated diodes shown have been used as "typical" unirradiated examples of results for all neutron, electron and gamma-ray irradiated diodes studied in the analysis of MRD500 diode C-f characteristics. The reported unirradiated values represent an average of four diodes taken from the same lot as all neutron, electron and gamma-ray irradiated diodes. The variation in averaged C-f measurements performed upon unirradiated diodes was typically ± 5% from the average. The uncertainty in all measured C-f data is estimated to be less than ± 10%.

CAPACITANCE (pF)

Freq. (Hz)	Pre-irradiation				3E12 γ/cm^2				3E13 γ/cm^2				3E14 γ/cm^2			
	V_R (volts)				V_R (volts)				V_R (volts)				V_R (volts)			
	0	5	10	20	0	5	10	20	0	5	10	20	0	5	10	20
10^2	6.98	4.00	2.96	2.88	6.81	3.94	2.92	2.78	6.53	3.61	2.76	2.67	4.98	3.07	2.51	2.25
10^3	6.98	4.00	2.96	2.88	6.81	3.94	2.92	2.78	6.52	3.62	2.76	2.67	4.97	3.06	2.51	2.25
10^4	6.98	4.00	2.96	2.88	6.81	3.94	2.92	2.78	6.52	3.62	2.76	2.67	4.97	3.06	2.52	2.25
10^5	6.98	4.00	2.96	2.88	6.81	3.94	2.92	2.78	6.52	3.61	2.76	2.67	4.97	3.06	2.51	2.25
10^6	6.98	4.00	2.96	2.88	6.81	3.94	2.92	2.78	6.52	3.61	2.76	2.67	4.97	3.06	2.51	2.25
10^7	6.98	4.00	2.96	2.88	6.81	3.94	2.92	2.78	6.52	3.61	2.76	2.67	4.97	3.06	2.51	2.25

TABLE 1 : Capacitance-frequency characteristics of pre-irradiated and gamma-ray irradiated MRD500 P-I-N diodes.

Gamma-ray irradiated MRD500 diode C-f characteristics shown in table 1 were obtained at various reverse bias voltages for several gamma-ray fluences. Tabulated experimental results indicate that at constant frequency, C_J decreases as V_R increases (up to approximately -10 V). Also, C_J decreases as gamma-ray fluence increases, for constant V_R and constant frequency. Finally, tabulated results show that for a constant irradiation level and reverse bias voltage, C_J remains essentially independent of frequency in the range from 100 Hz to 10 MHz.

Figures 12(a) and 12(b) show MRD500 diode C-f characteristics measured at several reverse bias voltages, for electron fluences of 4E14 e/cm^2 and 4E16 e/cm^2. The figures indicate that at a constant fluence and frequency, C_J decreases as V_R increases (up to approximately -10 to -20 V). Also, the figures indicate that a noticeable monotonic step-like decrease is seen in C_J with frequency, at both 4E14 e/cm^2 and 4E16 e/cm^2.

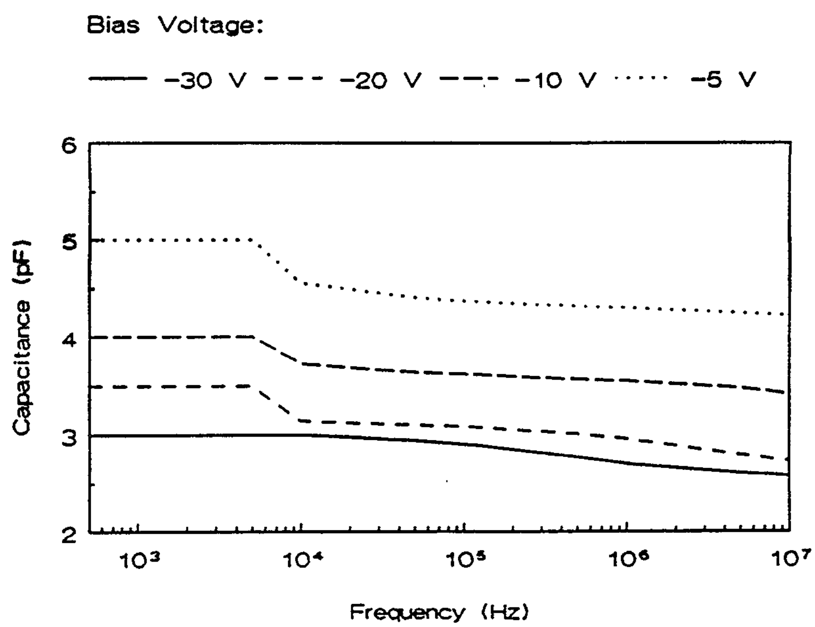

Figure 12(a) : **Capacitance-frequency characteristics of MRD500 diodes following irradiation with 4E14 e/cm^2.**

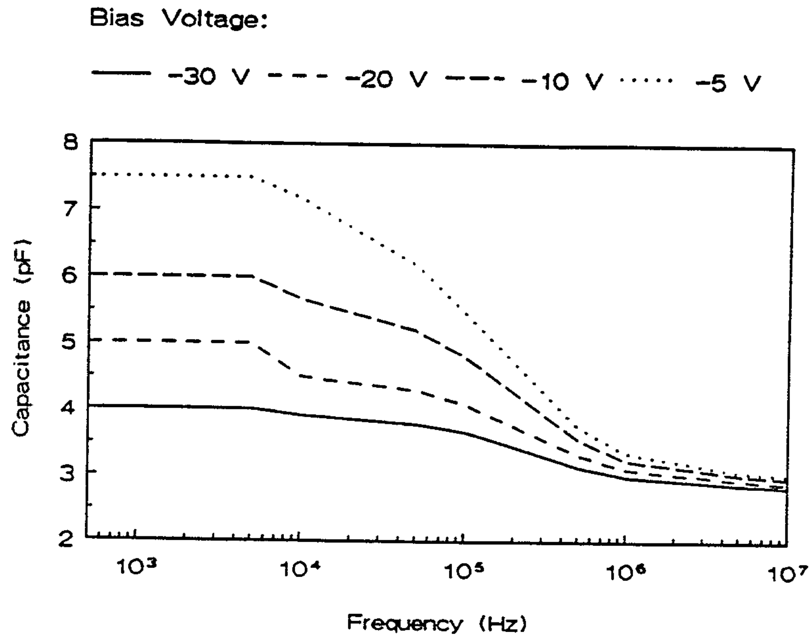

Figure 12(b) : **Capacitance-frequency characteristics of MRD500 diodes following irradiation with 4E16 e/cm^2.**

Figure 13 shows neutron irradiated MRD500 diode C-f characteristics for a neutron fluence of 1E15 n/cm^2, measured at several reverse bias voltages. This figure shows trends similar to those observed for gamma-ray and electron irradiated devices, especially the noticeable monotonic step-like decreases in C_J with frequency seen for the electron irradiated diodes of figures 12(a) and 12(b).

The frequency dependence of the junction capacitance of P-I-N diodes is a complex function[12,15-17] of dopant concentrations, pre- and post-irradiation defect concentrations, junction width, base region width, and frequency of the voltage signal applied to the device. The resultant description of this capacitance as a function of signal frequency, $C_J(\omega)$, is given[16] by

$$C_J(\omega) = C_{HF} + \frac{C_{HF} - C_{LF}}{1 + \omega^2 \tau_{eff}^2} \qquad (4.4)$$

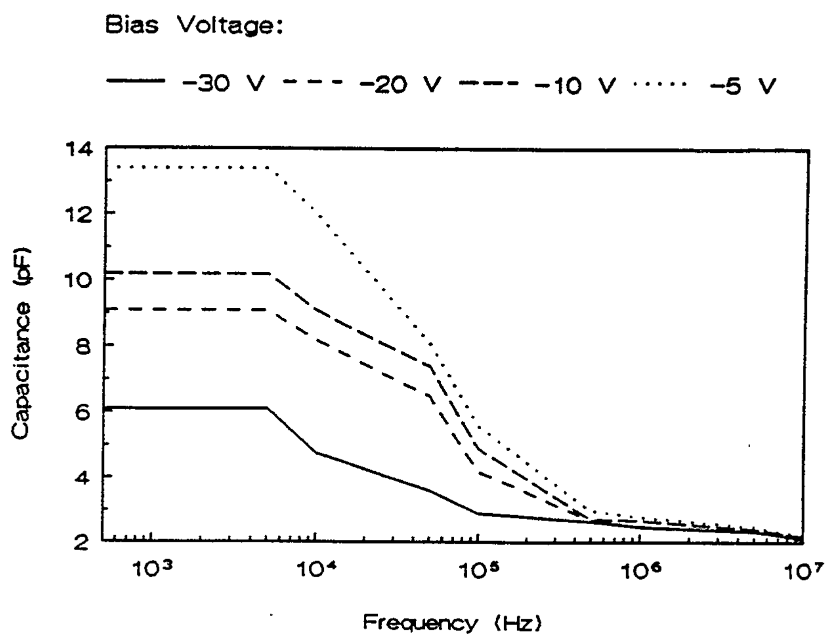

Figure 13 : **Capacitance-frequency characteristics of MRD500 diodes following irradiation with 1E15 n/cm^2.**

where

ω = the frequency of the applied signal (Hz, kHz, MHz...),

C_{HF} = the high-frequency limit of C_J , (equation (4.2)),

C_{LF} = the low-frequency limit of C_J, and

τ_{eff} = the effective relaxation time of charge carriers from the conduction band (MRD500) to defect sites in the base material of the semiconductor.

The effective relaxation time depends upon not only the physical relaxation time of the carriers and upon V_R , but also upon the actual concentration of the defects in which the carriers become "trapped". The low frequency capacitance is a complicated expression consisting of both real and imaginary components.

Pre-irradiation differences in C_{LF} and C_{HF} of P-I-N diodes have been found to be insignificant[17]. Therefore, for unirradiated diodes, equation (4.4) can be transformed[15] into either equation (4.2), when V_R exceeds the depletion voltage of the device, or into equation (4.3), when V_R remains less than the depletion voltage. Table 1 indicates that C_J decreases as voltage increases, up to $V_R \approx -10$ V. Beyond this point, C_J becomes essentially independent of applied V_R. Therefore, equation (4.3) describes the unirradiated MRD500 diode C-f behaviour up to -10 V, and equation (4.2) describes the behaviour for $V_R \leq -10$ V. Note that this behaviour is substantiated by results presented in section 4.4, where the depletion voltage of the MRD500 diode was found to be approximately -10 V. Therefore, the voltage and frequency-invariance of C_J for $V_R \leq -10$ V observed for unirradiated MRD500 diodes is not unexpected.

The post-irradiation C-f characteristics of MRD500 diodes shown in table 1 and in figures 12(a), 12(b) and 13 indicate that at constant fluence and frequency, for V_R less than approximately -10 V to -20 V (depletion voltage), C_J decreases as voltage increases. For the gamma-ray irradiated MRD500 diodes seen in table 1, C_J remains invariant with frequency. However, C-f characteristics of electron and neutron irradiated MRD500 diodes shown in figures 12(a), 12(b) and 13, respectively, indicate that a definite frequency dependence exists for C_J.

Equation (4.4) can be used to discuss the post-irradiation C-f characteristics of MRD500 diodes. At very high frequencies ($\approx$ GHz) and/or at very low device damage levels, equation (4.4) can be simplified to show that $C_J = C_{HF}$. Hence, depending upon the level of V_R applied to the device, resultant C-f behaviour will be given either by equation (4.2) or (4.3). Although gamma-ray irradiated MRD500 C-f characteristics listed in table 1 were not measured at GHz frequencies, the small $\Delta C_J(\phi)$ observed for the diodes (arising due to low device damage) thereby permit description of gamma-ray irradiated MRD500 C-f characteristics by equations (4.2) and (4.3).

At frequencies up to several MHz, the C_{LF} term shown in equation (4.4) dominates C_J, regardless of fluence. Hence, C-f characteristics observed for the electron and neutron irradiated MRD500 diodes of figures 12 through 13 are dominated by the C_{LF} term. In this regard, the complexity of the C_{LF} expression renders it impossible to predict electron and neutron irradiated MRD500 C-f characteristics. However, Dabrowski and Korbel[16,17] have provided an analytical method to describe qualitatively and quantitatively the C-f characteristics of moderately-to-highly irradiated P-I-N diodes containing radiation-induced displacement defect energy levels. Published experimental data[15-17] obtained using this method indicate the existence of a number of displacement defect energy levels, which results in the formation of an equivalent number of discrete reductions or "steps" in the C-f curve (at constant V_R) as the frequency of the voltage signal applied to the device under analysis is increased. Intuitively, shallow energy levels appear as relatively low frequency (≈ Hz) steps, while deep energy levels appear as relatively high frequency (≈ several MHz) steps.

The absence of steps in the gamma-ray irradiated MRD500 diode C-f characteristics shown in table 1 indicate that gamma-ray-induced displacement defect concentrations are relatively low, and so, the existence of well-defined defect levels cannot be inferred. However, the steps seen in the electron irradiated MRD500 diode C-f characteristics shown in figures 12(a) and 12(b) suggest the existence of radiation-induced displacement defect levels in the electron irradiated devices[16,17].

The experimental results shown in figure 13 depict the presence of neutron-induced displacement defect levels, similar to results seen for electron irradiated diodes. Although the results presented in table 1 do not indicate the presence of well-defined defect levels, gamma-ray fluences represented in these figures are orders of magnitude relatively less effective at producing displacement damage equivalent to that produced by the electron and neutron fluences[7,8] represented in figures 12(a), 12(b) and 13, respectively. Therefore, gamma-ray-induced displacement defect concentrations are commensurately lower than those induced by neutron and electron irradiation of the MRD500 diodes.

Note that C_J measurements were made for a wide range of frequencies, to ensure that the observed "steps" were not artifacts created during the measurement process.

4.6 CARRIER LIFETIME

Lifetime measurements described in section 3.6 were obtained for use as validation of $\Delta V_F(\phi)$ damage correlations presented in section 4.1. It was found that although the experimental method selected was reported to be useful for measurement of nanosecond lifetimes[21], meaningful lifetime measurements could not be obtained for the MRD500, which has a sub-nanosecond lifetime ($\tau_{RISE\ TIME} < 1$ ns). An alternate measurement technique must be developed to obtain lifetimes in very high-speed P-I-N junction diodes such as the MRD500.

5.0 CONCLUSIONS

The Motorola MRD500 photodiode is an abrupt P-I-N junction, narrow-base, fast device. Permanent changes in the electrical characteristics of the MRD500 diode following exposure to a range of fluences and energies of neutrons, electrons and gamma-rays are related primarily to displacement damage in these devices. Measurements of $\Delta V_F(\phi)$ at constant I_F and constant temperature were used to experimentally investigate the equivalence of neutron, electron and gamma-ray-induced displacement damage effects in MRD500 diodes, and to determine displacement damage correlations in silicon for the types and energies of radiation used in this work.

For constant forward current, MRD500 diode forward voltage decreases monotonically with increases in fluence; from 1E11 n/cm^2 (1 MeV equivalent) up to the reversal fluence of greater than 1E14 n/cm^2, from 4E12 e/cm^2 (7.5 MeV average energy) up to the reversal fluence of greater than 4E14 e/cm^2, and from 3E13 γ/cm^2 (1.25 MeV average energy) up to 3E15 γ/cm^2 (reversal fluence not reached). Specifically, since shifts in V_F remain linear for neutron fluences of up to 1E14 n/cm^2, the MRD500 diode is useful as a neutron fluence monitor well beyond the range (up to $\approx$ 1E12 n/cm^2) of the widely-used Harshaw DN-156 P-I-N diode neutron fluence monitors (currently used[22] by the Nuclear Effects Directorate at Aberdeen Proving Ground, Aberdeen, Md.). Following suggestions from the authors, the Nuclear Effects Directorate is presently investigating the suitability of the MRD500 diode as a neutron fluence monitor and as a flash x-ray pulse monitor.

Experimental measurements of fluences of 7.5 MeV electrons and 1.25 MeV gamma-rays required to produce (at constant current) a ΔV_F similar to the ΔV_F created by fluences of neutrons (1 MeV equivalent) were compared with published damage-equivalence results[7]. Published damage-equivalence results showed good agreement with experimentally-determined damage-equivalence results.

The MRD500 diode is currently being used at DREO as a calibration device for comparison of peak photocurrents generated in semiconductor devices by a given dose rate of electrons from a LINAC, with a given rate of energy deposition from photons generated by a pulsed infrared (1064 nm) Nd:YAG laser. It is desirable to reuse individual MRD500 diodes for multiple "shots" during experimental work if changes in the electrical characteristics of the device (i.e. device damage) do not detrimentally affect the measurement of photocurrent. Measurements of pre- and post-irradiation I-V characteristics and breakdown voltage characteristics of electron irradiated MRD500 diodes are, therefore, important to delimit the useful device lifetime (in terms of total electron fluence and/or total dose) for a given electron energy. Similarly, this information has application in determining the useful device lifetime for the MRD500 as a flash x-ray pulse monitor and as a neutron fluence monitor. Although infrared radiation from the Nd:YAG is incapable of producing displacement damage in the MRD500 diode (or in any other semiconductor material or device), changes in I-V characteristics of laser irradiated diodes can be used to indicate the onset of thermally induced damage to the devices. Measured data will be used at DREO to support ongoing experimental work in this area.

The investigation of radiation-induced changes in the electrical characteristics of MRD500 diodes could be extended to increase greatly the resolution of the currently existing $\Delta V_F(\phi)$ data for electron, neutron and gamma-ray irradiated devices. Also, gamma-ray irradiations could be performed at higher fluence levels (e.g. 3E16, 3E17 γ/cm^2), to define the reversal fluence for gamma-ray irradiated MRD500 diodes. Finally, an investigation of the short and long-term annealing behaviour of irradiated MRD500 diodes could be performed, to increase the repeatability and accuracy of all $\Delta V_F(\phi)$ measurements performed on MRD500 diodes. This data could be used to increase the accuracy of MRD500 P-I-N photodiode experimental displacement damage correlations obtained for neutrons, electrons and gamma-rays.

6.0 APPENDIX A - SEMICONDUCTOR JUNCTION CURRENT-VOLTAGE CHARACTERISTICS

The current-voltage characteristics of unirradiated, abrupt junction P-I-N diodes operating in low-level injection can be accurately approximated by the diode equation[2-4]

$$I_D = \frac{qAn_iW}{2\tau_0}\exp\left(\frac{qV_J}{2kT}\right) + I_S\left[\exp\left(\frac{qV_J}{kT}\right) - 1\right] \qquad (6.1)$$

where

I_D = diode forward (I_F) or reverse bias current (I_R),

I_S = diode reverse bias saturation current,

V_J = junction voltage,

n_i = intrinsic carrier concentration (approximately 10^{20} electrons and holes per cm^3 of intrinsic Si),

A = cross-sectional area of the junction,

W = width of the junction,

q = unit electronic charge

and

τ_0 = effective minority carrier lifetime within the junction region.

The first part of equation (6.1) describes the recombination component of the diode current, arising from the recombination of electrons and holes within the depletion region(s) of the diode. The second part is the diffusion component, arising from the recombination and subsequent diffusion of excess minority electrons and/or holes (injected from the external circuit through ohmic contacts) within the neutral semiconductor material of the diode. The I_S term is a constant that depends upon the physical and chemical properties of the semiconductor material. It has been shown[2,3] that for $V_R \leq -4kT/q$ ($V_R \approx -100$ mV at room temperature), I_R saturates at the limiting value I_S. Hence, I_S is defined as the diode reverse bias saturation current.

Specifically,

$$I_S = qA\left(\frac{D_h p_{no}}{L_h} + \frac{D_e n_{po}}{L_e}\right) \tag{6.2}$$

where

D_e , D_h = diffusion coefficient for electrons and holes, respectively,

L_e , L_h = diffusion length of electrons and holes, respectively

and

n_{po} , p_{no} = thermal equilibrium concentration of electrons (minority carriers) in the P-type material, and the thermal equilibrium concentration of holes (minority carriers) in the N-type material, respectively.

Since

$$n_{po} = \frac{n_i^2}{N_A} \tag{6.3}$$

and

$$p_{no} = \frac{n_i^2}{N_D} \tag{6.4}$$

then

$$I_S = qAn_i^2\left(\frac{D_h}{N_D L_h} + \frac{D_e}{N_A L_e}\right) \tag{6.5}$$

with

N_A = dopant level in the P-type material, and

N_D = dopant level in the N-type material.

Therefore, the complete diode equation is

$$I_D = qAn_i\left[\frac{W}{2\tau_0}\exp\left(\frac{qV_J}{2kT}\right) + n_i\left(\frac{D_h}{N_D L_h} + \frac{D_e}{N_A L_e}\right)\left(\exp\left(\frac{qV_J}{kT}\right)-1\right)\right] \qquad (6.6)$$

At room temperature, for forward bias voltages exceeding $8kT/q$ ($V_F \approx 200$ mV at room temperature), the diffusion component of the diode current dominates I_F and the diode equation becomes

$$I_F = qAn_i^2\left(\frac{D_h}{N_D L_h} + \frac{D_e}{N_A L_e}\right)\exp\left(\frac{qV_J}{kT}\right) \qquad (6.7).$$

For an unirradiated, abrupt junction, narrow-base P-I-N diode in which (for example) electron-type conduction dominates hole-type conduction[2] ($N_D > N_A$),

$$I_F = \frac{qAn_i^2 D_e}{N_A L_e}\exp\left(\frac{qV_J}{kT}\right) \qquad (6.8)$$

or

$$I_F = \frac{qAn_i^2\sqrt{D_e}}{N_A\sqrt{\tau_e}}\exp\left(\frac{qV_J}{kT}\right) \qquad (6.9)$$

since

$$L_e = \sqrt{D_e\tau_e} \qquad (6.10)$$

and with D_e and τ_e representing the diffusion coefficient and carrier lifetime for electrons, respectively. Solving for V_J ,

$$V_J = \frac{kT}{q} \ln\left[\frac{I_F N_A \sqrt{\tau_e}}{qAn_i^2 \sqrt{D_e}}\right] \tag{6.11}$$

Since the forward voltage drop across the diode, V_F , is

$$V_F = V_J + V_B \tag{6.12}$$

where V_B is the resistive voltage drop across the base region of the diode, then in P-I-N diodes with narrow, relatively low resistance base regions, most of the total forward voltage is dropped across the junction, V_J. Alternately, since the base resistance of the diode (and therefore, V_B) increases dramatically with the width of the base region, V_F is dominated by V_B for wide-base P-I-N junction diodes.

The unirradiated, reverse bias behaviour of abrupt junction, narrow-base P-I-N diodes is explained by examining I_R for various levels of reverse bias. Equation (6.6) defines the two components of diode reverse current; first, the generation component of I_R (analogous to the recombination component of I_F) arising from generation of electron-hole pairs in the depletion regions of the junctions of the device[2,3]; and second, the diffusion component of I_R , arising from processes similar to those described for forward biased diodes. At room temperature, for $V_R \leq -4kT/q$, the diffusion component dominates I_R and the diode equation becomes

$$I_R = I_S = qAn_i^2 \left(\frac{D_h}{N_D L_h} + \frac{D_e}{N_A L_e}\right) \tag{6.13}$$

Additionally, equations (6.10) and (6.13) show that for an abrupt junction, narrow-base P-I-N diode in which $N_D > N_A$,

$$I_R = qAn_i^2 \left(\frac{\sqrt{D_e}}{N_A \sqrt{\tau_e}}\right) \tag{6.14}$$

when $V_R \leq -4kT/q$. Analogous to equation (6.12), V_R can be described by

$$V_R = V_J + V_B \tag{6.15}$$

Therefore, since $V_J < V_B$, most of the total reverse voltage is dropped across the base of an unirradiated P-I-N diode with a narrow base region, as long as $V_R \leq -4kT/q$. Also, since the voltage dependence of I_R has been removed, I_R has effectively become "saturated" at I_S, and will remain relatively constant until V_R approaches the breakdown voltage of a device[2,3]. Hence, V_B dominates V_R across the operational range of reverse biases of the P-I-N diode.

7.0 REFERENCES

(1) S.M. Khanna, G.T. Pepper and R.E. Stone, "Neutron Radiation Induced Degradation of Diode Characteristics", Defence Research Establishment Report No. 1155, Ottawa, Canada, December 1992.

(2) A.S. Grove, **Physics and Technology of Semiconductor Devices**, John Wiley and Sons, Inc., New York, N.Y., 1967.

(3) S.M. Sze, **Physics of Semiconductor Devices**, John Wiley and Sons, Inc., New York, N.Y., 1969.

(4) R.J. Chaffin, **Microwave Semiconductor Devices: Fundamentals and Radiation Effects**, John Wiley and Sons, Inc., New York, N.Y., 1973.

(5) N.J. Rudie, **Principles and Techniques of Radiation Hardening, Vol. III, Third Edition**, Western Periodicals Company, North Hollywood, Ca., 1986.

(6) V.S. Vavilov and N.A. Ukhin, **Radiation Effects in Semiconductors and Semiconductor Devices**, Consultants Bureau (A Division of Plenum Press), New York, N.Y., 1977.

(7) C.J. Dale, P.W. Marshall, E.A. Burke, G.P. Summers, and E.A. Wolicki, "High Energy Electron Induced Displacement Damage in Silicon", IEEE Trans. Nucl. Sci., vol. NS-35, No. 6, December 1988.

(8) J.C. Garth and E.A. Burke, "Displacement Damage and Dose Enhancement in Gallium Arsenide and Silicon", IEEE Trans. Nucl. Sci., vol. NS-32, No. 6, December 1985.

(9) G.T. Pepper, S.M. Khanna, D. Snelling, and R.A. Sawchuk, "Nuclear Weapon Dose Rate Effects Simulation in Semiconductor Devices Using A Nd:YAG Laser", Defence Research Establishment Ottawa, Ottawa, Canada. Unpublished, 1991.

(10) R.J. Chaffin, "Permanent Neutron Damage in PIN Microwave Diode Switches", IEEE Trans. Nucl. Sci., vol. NS-18, No. 6, December 1971.

(11) V.A.J van Lint, T.M. Flanagan, R.E. Leadon, J.A. Naber, and V.C. Rogers, **Mechanisms of Radiation Effects in Electronic Materials, Volume 1**, John Wiley and Sons, New York, N.Y., 1980.

(12) M.G. Buehler, "The Space-Charge Region of Neutron -Irradiated $p^{+}n$ Junctions", IEEE Trans. Nucl. Sci., vol. NS-17, No. 6, December 1970.

(13) J.M. Swartz and M.O. Thurston, "Analysis of the Effect of Fast-Neutron Bombardment on the Current-Voltage Characteristic of a Conductivity-Modulated P-I-N Diode", Journal of App. Physics, vol. 37, No. 2, February 1966.

(14) M. Hasegawa, S. Mori, T. Ohsugi, H. Kojima, A. Taketani, T. Kondo, and M. Noguchi, "Radiation Damage of Silicon Junction Detectors by Neutron Irradiation", Nucl. Instr. and Meth. A277, pp. 395-400, 1989.

(15) W. Dabrowski and K. Korbel, "The Influence of Fast Neutron Irradiation on the Noise Performance of Silicon Surface-Barrier Detectors", Nucl. Instr. and Meth., A271, pp. 585-587, 1988.

(16) W. Dabrowski and K. Korbel, "Effects of Deep Imperfection Levels on the Capacitance of Semiconductor Detectors", Nucl. Instr. and Meth., A276, pp. 270-279, 1989.

(17) W. Dabrowski, K. Korbel, and A. Skoczen, "Fast Neutron Damage of Silicon PIN Photodiodes", Nucl. Instr. and Meth., A301, pp. 288-294, 1991.

(18) Motorola Optoelectronics Device Data, DL113, Rev. 3, Technical Information Center, Motorola Inc., 1989.

(19) Private communication with Motorola Technical Information Center, June 1991.

(20) Private Communication with J. Gerdes, Test and Research Division, Nuclear Effects Directorate, U.S. Army Combat Systems Test Activity, Aberdeen Proving Ground, Md., U.S.A., May 1991.

(21) R.H. Dean and C.J. Nuese, "A Refined Step-Recovery Technique for Measuring Minority Carrier Lifetimes and Related Parameters in Asymmetric P-N Junction Diodes", IEEE Trans. Elec. Dev., vol. ED-18, No. 3, March 1971.

(22) C.R. Heimbach, "The Use of Neutron-Sensitive Diodes as Monitors for 1-MeV Equivalent Neutrons", Test and Research Division, Nuclear Effects Directorate, U.S. Army Combat Systems Test Activity, Aberdeen Proving Ground, Md., August 1990.

UNCLASSIFIED

SECURITY CLASSIFICATION OF FORM
(highest classification of Title, Abstract, Keywords)

DOCUMENT CONTROL DATA

(Security classification of title, body of abstract and indexing annotation must be entered when the overall document is classified)

1. ORIGINATOR (the name and address of the organization preparing the document. Organizations for whom the document was prepared, e.g. Establishment sponsoring a contractor's report, or tasking agency, are entered in section 8.)
Defence Research Establishment Ottawa
Ottawa, Ontario
K1A 0Z4

2. SECURITY CLASSIFICATION (overall security classification of the document including special warning terms if applicable)
UNCLASSIFIED

3. TITLE (the complete document title as indicated on the title page. Its classification should be indicated by the appropriate abbreviation (S.C or U) in parentheses after the title.)
Neutron, Electron and Gamma-Ray Radiation Responses of a Fast P-I-N Photodiode (U)

4. AUTHORS (Last name, first name, middle initial)
Pepper, G.T., Khanna, S.M. and Stone, R.E.

5. DATE OF PUBLICATION (month and year of publication of document)
November 1994

6a. NO. OF PAGES (total containing information. Include Annexes, Appendices, etc.)
55

6b. NO. OF REFS (total cited in document)
22

7. DESCRIPTIVE NOTES (the category of the document, e.g. technical report, technical note or memorandum. If appropriate, enter the type of report, e.g. interim, progress, summary, annual or final. Give the inclusive dates when a specific reporting period is covered.
DREO Report

8. SPONSORING ACTIVITY (the name of the department project office or laboratory sponsoring the research and development. Include the address.
Defence Research Establishment Ottawa, 3701 Carling Avenue, Ottawa, Ontario, K1A 0Z4

9a. PROJECT OR GRANT NO. (if appropriate, the applicable research and development project or grant number under which the document was written. Please specify whether project or grant)
Project 041LS

9b. CONTRACT NO. (if appropriate, the applicable number under which the document was written)

10a. ORIGINATOR'S DOCUMENT NUMBER (the official document number by which the document is identified by the originating activity. This number must be unique to this document.)
DREO REPORT 1237

10b. OTHER DOCUMENT NOS. (Any other numbers which may be assigned this document either by the originator or by the sponsor)

11. DOCUMENT AVAILABILITY (any limitations on further dissemination of the document, other than those imposed by security classification)

(X) Unlimited distribution
( ) Distribution limited to defence departments and defence contractors; further distribution only as approved
( ) Distribution limited to defence departments and Canadian defence contractors; further distribution only as approved
( ) Distribution limited to government departments and agencies; further distribution only as approved
( ) Distribution limited to defence departments; further distribution only as approved
( ) Other (please specify):

12. DOCUMENT ANNOUNCEMENT (any limitation to the bibliographic announcement of this document. This will normally correspond to the Document Availability (11). however, where further distribution (beyond the audience specified in 11) is possible, a wider announcement audience may be selected.)
Unlimited Announcement

UNCLASSIFIED

SECURITY CLASSIFICATION OF FORM

UNCLASSIFIED

SECURITY CLASSIFICATION OF FORM

13. **ABSTRACT** (a brief and factual summary of the document. It may also appear elsewhere in the body of the document itself. It is highly desirable that the abstract of classified documents be unclassified. Each paragraph of the abstract shall begin with an indication of the security classification of the information in the paragraph (unless the document itself is unclassified) represented as (S), (C), or (U). It is not necessary to include here abstracts in both official languages unless the text is bilingual).

(U) This work is an experimental investigation of radiation-induced changes in the electrical characteristics of the MRD500 P-I-N photodiode, due to various fluences and energies of neutrons, electrons and gamma-rays. Analyses of changes in MRD500 forward bias current-voltage (I-V) characteristics, as a function of fission spectrum neutron fluence (reported as 1 MeV equivalent), indicate that the device can serve as a neutron fluence monitor, useable well beyond the range of the widely-used Harshaw DN-156 P-I-N diode fluence monitors. Furthermore, experimentally-determined changes in MRD500 forward voltage, $\Delta V_F(\phi)$, (at constant I_F and constant temperature) as a function of various energies and fluences of neutrons, electrons and gamma-rays, demonstrate the potential usefulness of the MRD500 as a displacement damage monitor.

(U) In this study, fission neutrons (1 MeV equivalent), 7.5 MeV (average energy) electrons and 1.25 MeV (average energy) gamma-rays are used to investigate the effectiveness of these radiations in producing displacement damage in the MRD500. The device physics responsible for the radiation-induced changes in the electrical characteristics of the diode is also discussed.

14. **KEYWORDS, DESCRIPTORS or IDENTIFIERS** (technically meaningful terms or short phrases that characterize a document and could be helpful in cataloguing the document. They should be selected so that no security classification is required. Identifiers, such as equipment model designation, trade name, military project code name, geographic location may also be included. If possible keywords should be selected from a published thesaurus. e.g. Thesaurus of Engineering and Scientific Terms (TEST) and that thesaurus-identified. If it is not possible to select indexing terms which are Unclassified, the classification of each should be indicated as with the title.)

Radiation effects on electronics
Radiation damage
Displacement damage
Silicon P-I-N diode
Neutron fluence monitor
Radiation damage equivalent

149436

NO. OF COPIES NOMBRE DE COPIES	COPY NO. COPIE N°	INFORMATION SCIENTIST'S INITIALS INITIALES DE L'AGENT D'INFORMATION SCIENTIFIQUE
1	1	JB
AQUISITION ROUTE FOURNI PAR	DREO	
DATE	02 Feb 95	
DSIS ACCESSION NO. NUMÉRO DSIS		

DND 1158 (6-87)

National Defence / Défense nationale

PLEASE RETURN THIS DOCUMENT TO THE FOLLOWING ADDRESS:

DIRECTOR
SCIENTIFIC INFORMATION SERVICES
NATIONAL DEFENCE
HEADQUARTERS
OTTAWA, ONT. - CANADA K1A 0K2

PRIÈRE DE RETOURNER CE DOCUMENT À L'ADRESSE SUIVANTE:

DIRECTEUR
SERVICES D'INFORMATION SCIENTIFIQUES
QUARTIER GÉNÉRAL
DE LA DÉFENSE NATIONALE
OTTAWA, ONT. - CANADA K1A 0K2